DOI 10.1007/s10946-023-10171-5
Journal of Russian Laser Research, Volume 44, Number 6, November, 2023

EFFECT OF GEOMETRIC PARAMETERS OF METALLIC NANOPRISMS ON THE PLASMONIC RESONANCE WAVELENGTH

Alexey D. Kondorskiy* **and Arseniy V. Mekshun**

Lebedev Physical Institute, Russian Academy of Sciences
Leninskii Prospect 53, Moscow 119991, Russia

*Corresponding author e-mail: kondorskiy@lebedev.ru

Abstract

We study the effect of geometric dimensions on the optical properties of equilateral triangular gold and silver nanoprisms with rounded corners. An analytical expression for calculating the spectral characteristics of the main longitudinal plasmonic resonance of such nanoprisms is obtained. As variables, the expression includes the nanoprism dimensions, its composition, and the permittivity of the surrounding environment. Our results demonstrate that the extinction cross sections can be adequately described by this expression for nanoprisms with edge lengths up to a few hundred nanometers. We show that the scattering of free electrons from the metal/environment interface in metallic nanoprisms can be described with the help of the size-dependent dielectric function. Using a simple relation, we evaluate the necessary effective size parameter, which allows one to achieve a good agreement with experimental data. The results obtained are of interest for solving a number of fundamental problems in nanophotonics and nanoplasmonics, as well as for applications in the development of next-generation optoelectronic devices.

Keywords: nanophotonics, nanoplasmonics, nanoprism, light extinction spectra, localized plasmon resonances, size and shape effects.

1. Introduction

Due to the intense development of nanophotonics and nanoplasmonics, a large number of recent works have been devoted to the study of optical properties of metallic nanostructures of different shapes [1–4]. Effects of the light interaction with such nanoparticles are explained in terms of localized surface plasmon resonances, which are responsible for strong enhancement of local electric fields near their surfaces, as well as the light absorption and scattering cross sections. Because of these unique properties, metallic nanostructures are being exploited in a wide range of applications including energy storage, sensing, catalysis, imaging, biotechnology [5–8]. The optical properties of metallic nanostructures of simple geometric shape (sphere, spheroid, cylinder, and disk) and the effects of their interaction with light have been intensely studied in many works; see [9–15] and references therein. More recently, metallic nanoparticles of more complex geometric shapes, such as triangular prisms, stars, pyramids, and some other anisotropic plasmonic nanoparticles have been controllably fabricated and investigated [16–22]. Intense studies of the optical properties of sharp-edged nanostructures (nanorods, nanotriangles, and nanostars) are stimulated by their applications for surface enhanced Raman scattering (SERS) [23].

Manuscript submitted by the authors in English on October 11, 2023.

In this work, we study the dependence of the optical properties of silver and gold equilateral triangular nanoprisms with rounded corners on their geometric parameters. The size and shape of typically synthesized triangular nanoprisms are characterized by three principal dimensions: edge length L, thickness H, and corner radius R; see Fig. 1. The spectra of such nanostructures strongly depend on all these parameters. The most sensitive to variation of nanoprism sizes is the main longitudinal plasmonic band. This band shows up in optical spectra, when the light polarization is parallel to the plane of the nanoprism base, XY plane in Fig. 1. This resonance band exhibits the red shift with increasing the edge length L [16–18].

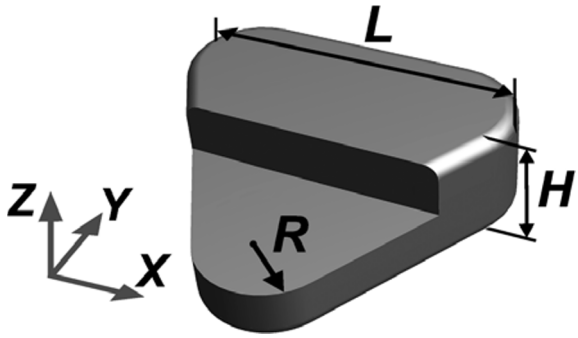

Fig. 1. Schematic view of the equilateral triangular nanoprism with rounded corners.

The other dimension is the triangle corner radius R. Depending on the specific method of nanostructure synthesis, this parameter can vary significantly. The gold nanoprisms synthesized in [16] have essentially sharp edges, i.e., R is negligible compared to H and L. The silver nanoprisms synthesized in [18] have a radius of $R \sim 4$ nm. As we show below; see Sec. 3., the main longitudinal plasmonic band blue-shifts with increase in the radius R and the shift value can be essentially large. For the nanoprism with sizes close to that studied in [18], the shift is about 40 nm, which exceeds the plasmonic resonance half-width; see Sec. 3. and Fig. 2 a.

To describe the influence of the dimensions of a plasmonic nanostructure on its optical properties, it is convenient to use a semi-empirical universal analytical model first introduced in [24]. As shown in [25], the model can be applied to plasmonic nanoparticles of different shapes. Plasmonic band broadening and red-shifts due to retardation [10, 24, 25] are also included in the model. The dipole polarizability, extinction, and scattering spectrum of a particle can be effectively represented by just a few numerical values. These values are solely determined by the particle shape and are independent of the average size, permittivity of the particle, and the host material. By systematical analysis of the relationship between these parameters and the dimensions of a specific particle shape, one can develop an appropriate analytical expression for the calculation of the spectral properties of a plasmonic nanoparticle.

The theoretical study of the plasmonic resonances of triangular nanoprisms, using the analytical model, was performed in [25], where it was assumed that $R \ll H$ and $R \ll L$. The analytical expression presented there depends only on the parameters L and H. However, the plasmonic resonance wavelength also depends on the radius R.

In this work, we obtain the parameters for the analytical expression that can be used to calculate the spectral characteristics of the main longitudinal plasmonic band of a nanoprism as a function of its three principal dimensions: the edge length L, the thickness H, and the corner radius R. We also consider the effect associated with free-electron scattering at the metal/environment interface. This effect has been studied for spherical nanoparticles in terms of the phenomenological size-dependent dielectric function of the metal [12, 13, 15]. Recently, the importance of considering this effect for a proper theoretical description of the optical properties of nanostars has been pointed out in [26]. Here, we evaluate the dielectric function size parameter for the case of non-spherical shape of nanoparticles. The computer code developed in this work to perform the calculations with the obtained analytical expression is published as open source on GitHub [27].

2. Theoretical Approach

We perform numerical simulation of light extinction and scattering processes by the plasmonic nanoprisms, using the finite-difference time-domain (FDTD) method implemented in a freely available software package MIT Electromagnetic Equation Propagation (MEEP). The details of the calculation method can be found in [20]. The optical properties of the materials comprising the nanostructures under study are determined by their dielectric functions. We describe here the dielectric functions of silver and gold nanoparticles similarly to works [12,13,15,20,28], taking into account the contributions of free and bound electrons and the size effect caused by electron scattering from the metal/environment interface. We use the phenomenological approach [29, 30]. The frequency and size-dependent dielectric function $\varepsilon_m(\omega, D)$ of a metallic nanoparticle can be written as

$$\varepsilon_m(\omega, D) = \varepsilon_m^{\text{bulk}}(\omega) + \omega_{\text{p}}^2 \left(\frac{1}{\omega^2 + i\omega\gamma_{\text{intra}}^{\text{bulk}}} - \frac{1}{\omega^2 + i\omega\gamma_{\text{intra}}(D)} \right). \tag{1}$$

Here, D is the size of the particle, $\varepsilon_m^{\text{bulk}}(\omega)$ is the frequency-dependent dielectric function of a bulk metal sample, ω_p is the plasma frequency, $\gamma_{\text{intra}}^{\text{bulk}} = v_F/l_\infty$ is the damping constant in a bulk metal, v_F is the Fermi velocity, l_∞ is the electron mean free path. The effective size-dependent damping constant reads

$$\gamma_{\text{intra}}(D) = \gamma_{\text{intra}}^{\text{bulk}} + \zeta \frac{v_F}{D}. \tag{2}$$

For silver and gold, the values of $\varepsilon_m^{\text{bulk}}(\omega)$ have been reconstructed from the available experimental data in [31] and [32], respectively. The rest of the parameters are taken from [33]. For silver, $\omega_p = 9.1$ eV, $v_F = 1.39 \cdot 10^8$ cm/s, $l_\infty = 5.2 \cdot 10^{-6}$ cm, and $\zeta = 5$. For gold, $\omega_p = 9.0$ eV, $v_F = 1.38 \cdot 10^8$ cm/s, and $l_\infty = 1.28 \cdot 10^{-6}$ cm, $\zeta = 4$. Equations (1) and (2) are discussed in detail in [12,13,15].

The dielectric function defined by Eqs. (1) and (2) is shown to accurately describe the size effect in spherical nanoparticles, where the size D is the diameter of a sphere. To extend these expressions to nanoprisms, we take D to be the diameter of a sphere with the same volume as a target nanoprism. The prism volume is approximately given by

$$V = \frac{\sqrt{3}}{4} L^2 H. \tag{3}$$

The corresponding size D is

$$D = 2 \left(\frac{3V}{4\pi} \right)^{1/3} = 2 \left(\frac{3\sqrt{3}}{16\pi} L^2 H \right)^{1/3}. \tag{4}$$

Using the numerical FDTD method, it is possible to evaluate the cross sections for a given polarization of the incident radiation. We denote by σ_α the cross section obtained for the case, where the electric field is directed along the α axis, with $\alpha = X, Y, Z$; see Fig. 1. Here, we are particularly interested in the spectral properties of the large longitudinal plasmonic band. This band appears in optical spectra, when the light polarization is parallel to the plane of the nanoprism base as the XY plane in Fig. 1. An important result of our calculations is that, for a nanoprism with an equilateral triangular base, one has $\sigma_X \approx \sigma_Y$. Thus, to obtain the spectral parameters of this band, it is sufficient to calculate only a single value of σ_X or σ_Y. In this work, we present the results of the calculations of the extinction cross sections $\sigma_X^{(\text{ext})}$. It should be noted that, in the solutions, the nanoprisms are randomly oriented, so the measured cross section is an average over the possible orientations of the nanostructure, $\sigma = (\sigma_X + \sigma_Y + \sigma_Z)/3$.

Typically, however, the spectral features of the nanoprisms associated with $\sigma_X \approx \sigma_Y$ and σ_Z lie in well-separated wavelength regions, so that the main longitudinal plasmonic band can be well distinguished.

To describe the dependence of the optical properties of a plasmonic nanostructure on its dimensions, it is convenient to use a semi-empirical universal analytical model. In notation similar to those of review [25], the dipole polarizability of a plasmonic band has the form

$$\alpha = \frac{1}{4\pi} \frac{V\beta}{\dfrac{1}{\varepsilon_m/\varepsilon_h - 1} - \dfrac{1}{\varepsilon_c - 1} - A_{\rm rc}}, \tag{5}$$

where ε_m and ε_h are permittivity of the metal and the host media, respectively. The volume V is given by Eq. (3). The retardation correction can be written as [25]

$$A_{\rm rc} = a_2 s^2 + i\frac{4\pi^2 V\beta}{3L^3} s^3 + a_4 s^4, \tag{6}$$

where $s = \sqrt{\varepsilon_h} L/\lambda$ and λ is the light wavelength in vacuum. The associated extinction cross section is defined by the expression,

$$\sigma^{(\rm ext)} = 4\pi k_h \,{\rm Im}(\alpha), \tag{7}$$

while the corresponding scattering cross section is given by

$$\sigma^{(\rm scat)} = \frac{8\pi}{3} k_h^4 |\alpha|^2. \tag{8}$$

The wave vector of light in host media is $k_h = 2\pi\sqrt{\varepsilon_h}/\lambda$.

To obtain the parameters ε_c, β, a_2, and a_4 for the triangular nanoprisms, we calculate the extinction and scattering cross sections for the case of an incident electromagnetic wave polarized along the X axis and minimize the residual between the numerical results and the results of analytical expressions. For each set of nanoprism sizes, we fit the main longitudinal plasmonic band with Eqs. (5)–(8). The fitting procedure consists of two steps. First, the extinction cross sections are calculated for nanoprisms of small sizes, $L = 10$ nm, $H = 1 - 4$ nm, and $R = 1 - 4$ nm. For such small nanostructures, the quasistatic approximation is valid, so that the retardation correction $A_{\rm rc}$ can be neglected. These data are used to fit two parameters ε_c and β. Note that the parameter ε_c affects the wavelength of the cross section maximum, while β affects its maximum value.

As the nanoprism size increases, the parameters a_2 and a_4 begin to contribute to Eqs. (5)–(8). They affect the wavelength of the cross section maxima, so that we use the same procedure to fit them as for ε_c. To evaluate a_2 and a_4, we calculate the cross sections for nanoprisms of the medium size ($L = 30$ nm, $H = 3 - 12$ nm, and $R = 1 - 12$ nm) and of sufficiently large size ($L = 90$ nm, $H = 10 - 40$ nm, and $R = 4 - 40$ nm), respectively. After obtaining the parameters ε_c, β, a_2, and a_4 for a large number of sizes $[L, H, R]$, the dependence of each parameter on the nanoparticle dimensions is approximated by the expression

$$f(L,H,R) = C_1 \left(\frac{L}{H}\right)^{C_2} + C_3 \left(\frac{L}{R}\right)^{C_4} + C_5 \left(\frac{H}{R}\right)^{C_6} + C_7, \tag{9}$$

where C_n coefficients are determined to best fit the dependence of each parameter on the particle sizes. They are presented in Table 1. Also we developed the computer code to perform the calculations with

the obtained analytical expression, including the size-dependent dielectric function for silver and gold, and published it as open source on GitHub [27].

Table 1. The values of Coefficients C_n Used to Calculate the Parameters in Eqs. (5), (6), and (9).

	C_1	C_2	C_3	C_4	C_5	C_6	C_7
ε_c	−1.740	0.9049	23.70	−9.720	3.737	−0.4162	−4.234
β	−0.6495	−1.278	1.877	−0.9282	0.07846	−0.6196	0.6171
a_2	1.352	−0.5565	1.138	−0.4836	−0.2879	−0.4687	−0.05640
a_4	−2.588	−0.4472	−2.629	−2.973	−0.2549	−0.1255	0.7025

3. Results and Discussions

In Fig. 2, we show the light extinction cross sections $\sigma_X^{(\mathrm{ext})}$ by silver nanoprisms of different sizes in a water environment as functions of the light wavelength in vacuum. The results are obtained, using the analytical expression (curves B, D, and F) and the numerical calculations (curves A, C, and E). In Fig. 2, the edge lengths of the nanoprisms are $L = 20$ nm (a), $L = 50$ nm (b, c), and $L = 100$ nm (d–f). The values of the ratio of the nanoprism thickness to its edge length are as follows: $H/L = 0.1$ (d), $H/L = 0.2$ (b, e), $H/L = 0.4$ (c, f), and $H/L = 0.5$ (a). The results for very thin platelets, $H < 10$ nm, are not shown here, since they are hardly available for the experiments. In each figure, curves A and B show the results for small relative values of $R/L \leq 0.05$, curves C and D, for values of $R/L = 0.2$, and curves E and F, for large values of $R/L = 0.4$; the maximum possible value is $R/L = 0.5$. These figures allow us to follow the changes in the extinction spectra with increasing edge length L for fixed ratios H/L and R/L. The curvature radius of the nanoprism edges is kept negligible $\sim 0.01\,L$ in all cases under consideration.

In Figs. 3 and 4, we demonstrate the results of our calculations for gold and silver nanoprisms embedded in water and benzene, respectively. These calculations were performed using the same nanoprism sizes as shown in Fig. 2. As is evident from Figs. 2–4, the results obtained by our analytical expression are in quantitative agreement with the results of numerical calculations for a wide range of nanoprism sizes, aspect ratios, materials, and host permittivities. The expression accurately describes both the wavelength and the width of the plasmonic band. It also predicts the maximum values of the extinction cross sections, with a relative error of smaller than 15%.

We also calculate light extinction cross sections by large silver and gold nanoprisms; see Fig. 5. Here, the edge lengths are $L = 200$ nm and $L = 400$ nm (top and bottom rows). The H/L ratios are 0.1 (first and third columns) and 0.2 (second and fourth columns). Two pairs of curves are shown as A and B for $R = 5$ nm ($R \ll L$), and C and D for $R/L = 0.4$, essentially large value. The results for silver and gold are shown in the first and second columns, and the third and fourth columns, respectively.

Two key points should be made about the results shown in Fig. 5. First, the analytical expression still works for L up to 200 nm and loses its accuracy for L about 400 nm. Second, for large edge length $L = 400$ nm, the difference in plasmonic band wavelengths caused by different values of R disappears. The plasmonic resonance becomes broad enough to blur the difference in extinction spectra of nanoprisms with different aspect ratios.

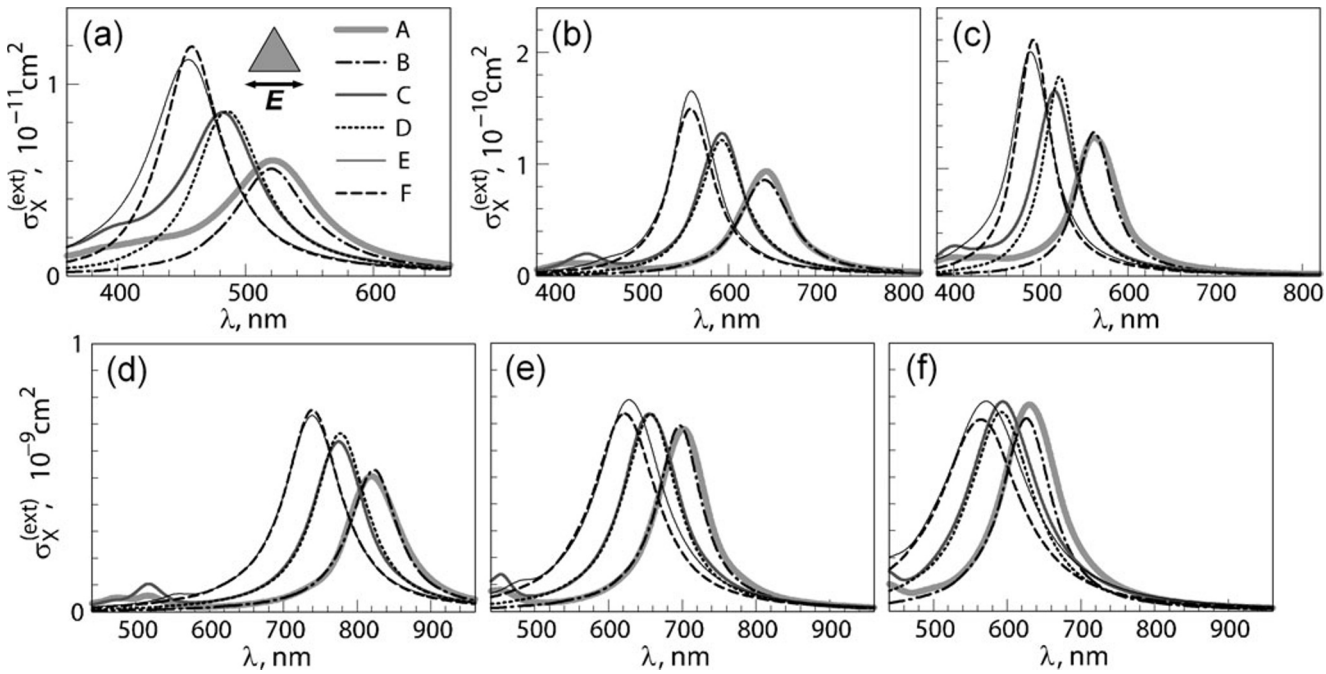

Fig. 2. Light extinction cross section calculated numerically and using the analytical expression for silver nanoprisms of different sizes embedded in water, $\varepsilon_h = 1.78$. The polarization of the incident radiation is directed along the X axis, as shown in Fig. 1. The solid thick gray curve (A), solid dark gray (C), and solid thin black (E) curves show numerical results. Dash-dotted black (B), dotted (D), and solid thin (E) curves show results obtained, using the analytical expression. In each figure, the results are shown for three values of $R = R_1$, R_2, and R_3. Curves A and B show results for $R = R_1$, curves C and D for $R = R_2$, and curves E and F for $R = R_3$. Here, face sizes $L = 20$ nm, $R_1 = 1$ nm, $R_2 = 4$ nm, and $R_3 = 8$ nm (a), $L = 50$ nm, $R_1 = 2$ nm, $R_2 = 10$ nm, and $R_3 = 20$ nm (b, c), and $L = 100$ nm, $R_1 = 5$ nm, $R_2 = 20$ nm, and $R_3 = 40$ nm (d–f). Also, the thickness $H = 10$ nm (a, b, d), $H = 20$ nm (c, e), and $H = 40$ nm (f).

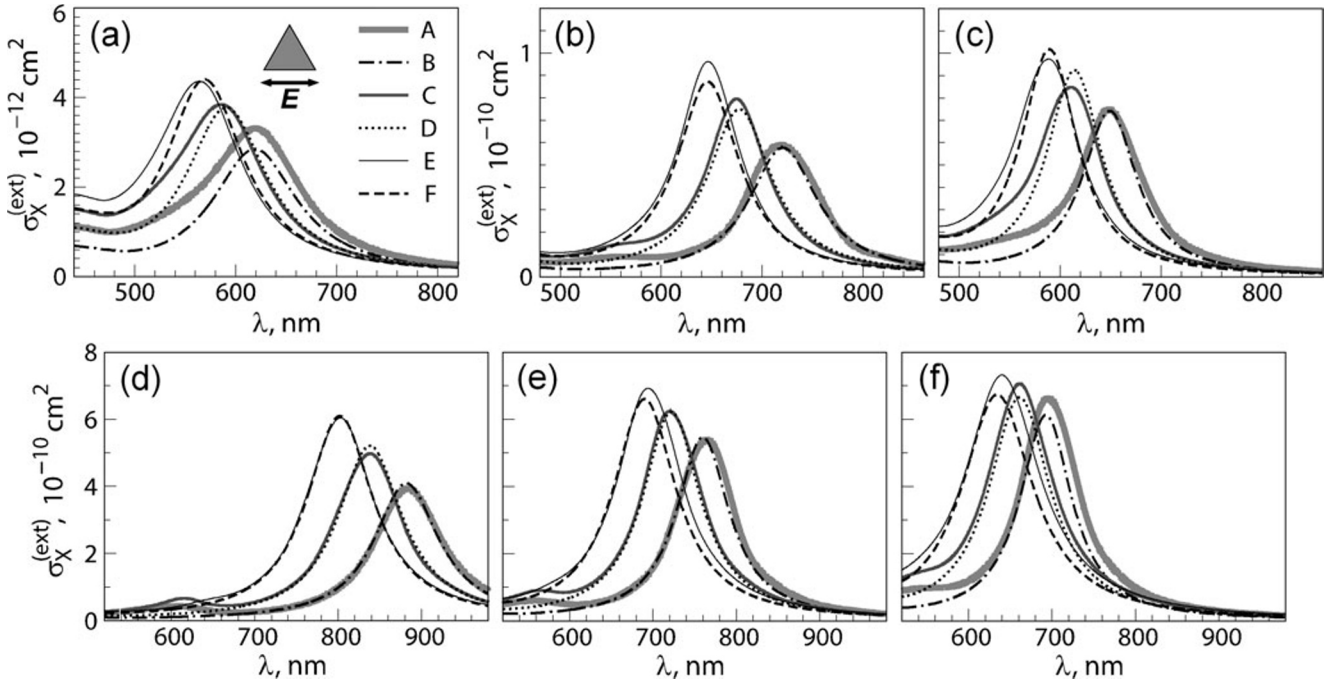

Fig. 3. The same as in Fig. 2 but for gold nanoprisms embedded in water, $\varepsilon_h = 1.78$.

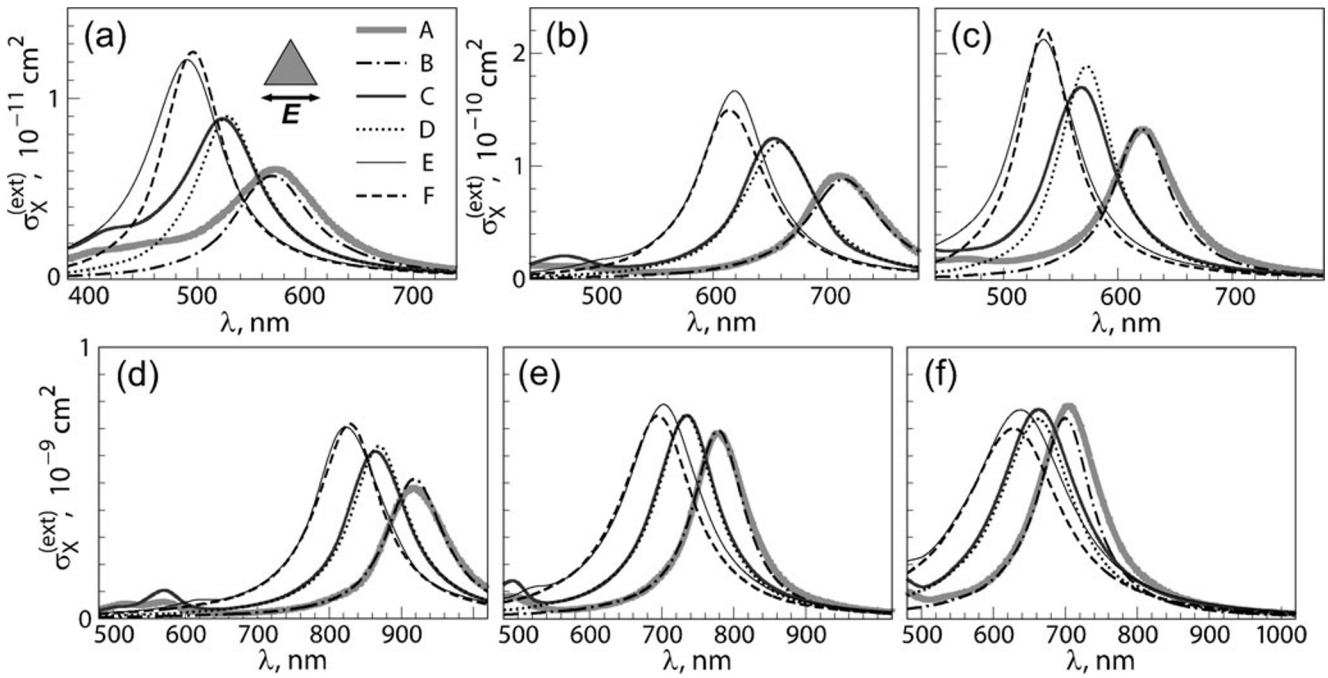

Fig. 4. The same as in Fig. 2 but for silver nanoprisms embedded in benzene, $\varepsilon_h = 2.274$.

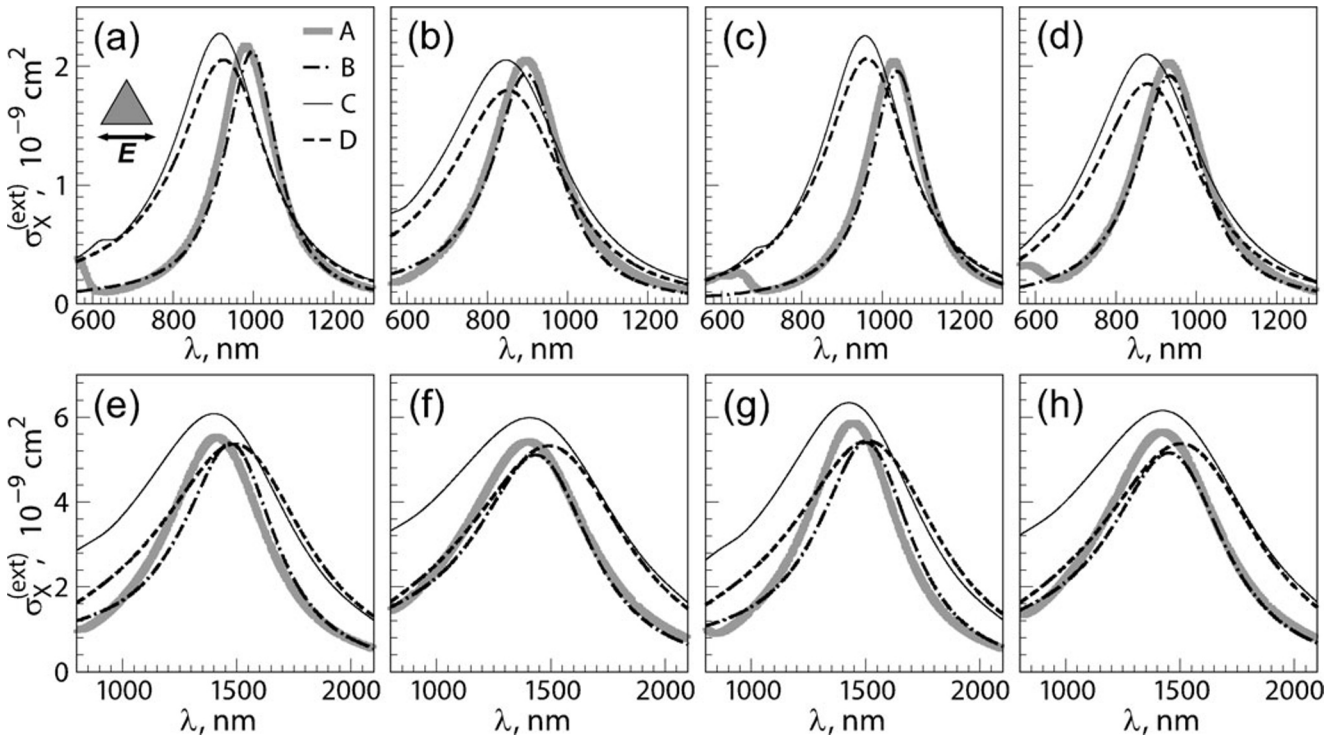

Fig. 5. Light extinction cross section calculated numerically and using the analytical expression for large silver and gold nanoprisms embedded in water, $\varepsilon_h = 1.78$. The polarization of the incident radiation is directed along the X axis, as shown in Fig. 1. The solid thick gray (A) and solid thin black (C) curves show numerical results. The dash-dotted (B) and dashed (D) curves show the results obtained, using the analytical expression. In each figure, the results are shown for two values of $R = R_1$ and R_2. Curves A and B show results for $R = R_1$, and curves C and D, for $R = R_2$. Nanoprism materials are silver (a, b) and (e, f) and gold (c, d) and (g, h). Here, face sizes $L = 200$ nm, $R_1 = 5$ nm, and $R_2 = 80$ nm (a, d) and $L = 400$ nm, $R_1 = 5$ nm, and $R_2 = 160$ nm (e, h). Also, the thickness $H = 20$ nm (a, c), $H = 40$ nm (b, d, e, h), and $H = 80$ nm (f, h).

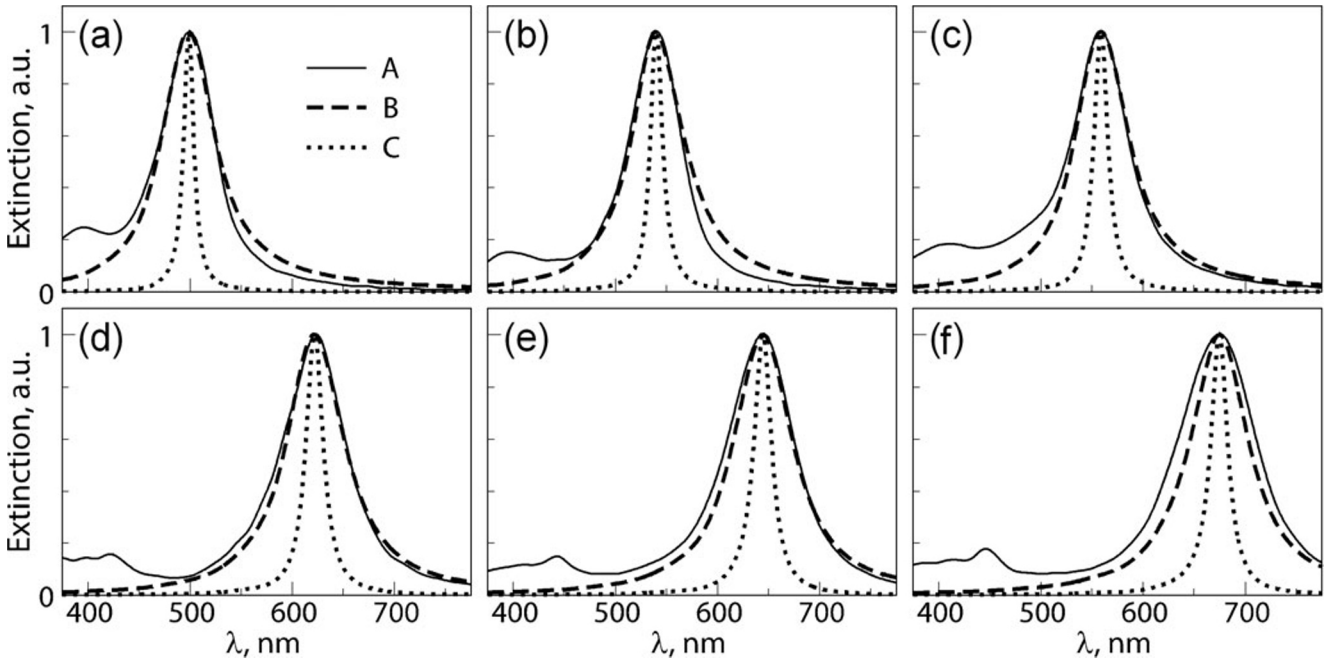

Fig. 6. Normalized light extinction by aqueous solution of silver nanoprisms. Here, the experimental data [18] (solid thin black curves A), the results obtained with analytical expression with size-dependent dielectric function of silver (dashed curves B), and the results obtained with the analytical expression using the dielectric function of bulk silver (dotted curves C). Also, sizes used in theoretical calculations $H = 10$ nm and $R = 4$ nm for all cases, the edge length $L = 23$ nm (a), $L = 31$ nm (b), $L = 35$ nm (c), $L = 49$ nm (d), $L = 54$ nm (e), and $L = 61$ nm (f).

Further, we compare the results calculated using our analytical expressions with the experimental data on the extinction spectra of aqueous solution of silver nanoprisms [18]. The results are presented for the nanoprism sizes designated in [18] as AgPRs-500, AgPRs-540, AgPRs-560, AgPRs-625, AgPRs-645, and AgPRs-675; they are shown in Fig. 6. The range of estimates for L obtained from the TEM images of the experimental samples are [18]: AgPRs-500: 25 ± 3 nm (a), AgPRs-540: 30 ± 4 nm (b), AgPRs-560: 33 ± 5 nm (c), AgPRs-625: 44 ± 9 nm (d), AgPRs-645: 47 ± 10 nm (e), and AgPRs-675: 52 ± 7 nm (f). The thickness of $H = 10$ nm is the same in all cases. Since the edge lengths L of the nanoprisms are determined from the TEM images within a certain range of estimates, we fit the values of L for each prism by matching the analytically calculated plasmonic band wavelength with that of the experimental extinction maxima. It is assumed that the corner radius R for all nanoprisms is 4 nm. Note that the values of L estimated by the analytical formula are in the range of the estimates, except for the last case.

As one can see in Fig. 6, the results obtained with size-dependent dielectric function, Eqs. (1) and (2), with effective size estimated from Eq. (4), demonstrate significant plasmonic band broadening compared to that obtained with bulk dielectric function of silver. The bandwidth obtained with the size-dependent dielectric function is in good agreement with the experimental data for all six samples, although the effective size estimated from Eq. (4) increases almost twofold from 16 nm (Fig. 6 a) to 31 nm (Fig. 6 f). Thus, our results clearly demonstrate the importance of using the size-dependent dielectric function in calculations of the extinction cross sections of plasmonic nanoparticles of complex shapes.

4. Conclusions

In this work, we studied the dependence of the spectral properties of the main longitudinal plasmonic resonance on three dimensions of an equilateral nanoprism, with rounded corners, edge length, thickness, and corner radius. We showed that the wavelength of this plasmonic band depended not only on the length/thickness ratio, but also on the radius/length and radius/thickness ratios. This is important because the corner radius can be changed significantly, depending on the specific method of nanostructure synthesis, so that the corresponding wavelength shift can exceed the plasmonic resonance half-width.

To describe the influence of the plasmonic nanoprism dimensions on its optical properties, we used a semi-empirical analytical model. The parameters of this universal model are solely determined by the particle shape and are independent of its average size and the permittivity, as well as the permittivity of the host material. We fitted the dependences of these model parameters on the three nanoprism dimensions mentioned above, using a simple formula. The resulting analytical expression can be used to evaluate the light extinction and scattering cross sections by a nanoprism of given sizes with negligible computational time. We showed that the obtained expression provided an adequate description of the cross sections for nanoprisms, with edge lengths of up to a few hundred nanometers.

We also considered the effect associated with free-electron scattering at the metal/environment interface. Recently, this effect has been studied for spherical nanoparticles in terms of the phenomenological size-dependent dielectric function of the metal. In this work, we showed that this approach can be applied to the case of non-spherical shape of nanoparticles. We presented a simple relation to evaluate the necessary effective size parameter, which allowed one to achieve a good agreement with the experimental data for the extinction spectra of silver nanoprisms.

We developed the computer code to perform the calculations with the obtained analytical expressions and published it as open source on GitHub [27]. We hope that this code will be a useful tool for fast and reliable evaluation of the spectral parameters of metallic nanoprisms and will help in preliminary analysis of experimental spectra of plasmonic nanoprisms.

Acknowledgments

This work was supported by the Russian Science Foundation under Grant No. 19-79-30086. The authors thank Prof. V. S. Lebedev and Dr. A. A. Narits for valuable discussions.

References

1. J. Pitarke, P. Xu, X. Yang, et al., *Rep. Prog. Phys.*, **70**, (2006); DOI: 10.1088/0034-4885/70/1/R01
2. N. J. Halas, S. Lal, W.-S. Chang, et al., *Chem. Rev.*, **111**, 3913 (2011); DOI: 10.1021/cr200061k
3. A. P. Pushkarev and M. N. Bochkarev, *Russ. Chem. Rev.*, **85**, 1338 (2016); DOI: 10.1070/RCR4665
4. N. G. Khlebtsov, L. A. Dykman, and B. N. Khlebtsov, *Russ. Chem. Rev.*, **91**, RCR5058 (2022); DOI: 10.57634/RCR5058
5. W. Ou, B. Zhou, J. Shen, et al., *Science*, **24**, 101982 (2021); DOI: 10.1016/j.isci.2020.101982
6. M. Seyyedi, A. Rostami, S. Matloub, *Opt. Quant. Electron.*, **52**, 308 (2020); DOI: 10.1007/s11082-020-02417-2
7. S. A. Bansal, V. Kumar, J. Karimi, et al., *Nanoscale Adv.*, **2**, 3764 (2020); DOI: 10.1039/D0NA00472C
8. A. U. Khan, Y. Guo, X. Chen, and G. Liu, *ACS Nano*, **13**, 4255 (2019); DOI: 10.1021/acsnano.8b09386

9. C. F. Bohren and D. R. Huffman, *Absorption and Scattering of Light by Small Particles*, Wiley, Weinheim (2004).
10. N. G. Khlebtsov, *J. Quant. Spectrosc. Radiat. Transf.*, **280**, 108069, (2022); DOI: 10.1016/j.jqsrt.2022.108069
11. L. Smitha, K. G. Gopchandran, T. R. Ravindran, and V. S. Prasad, *Nanotechnology*, **22**, 265705 (2011).
12. V. S. Lebedev, A. G. Vitukhnovsky, A. Yoshida, et al., *Colloids Surf. A Physicochem. Eng. Asp.*, **326**, 204 (2008); DOI: 10.1016/j.colsurfa.2008.06.027
13. V. S. Lebedev and A. S. Medvedev, *Quantum Electron.*, **42**, 701 (2012); DOI: 10.1070/qe2012v042n08abeh014833
14. A. D. Kondorskiy, K. S. Kislov, N. T. Lam, and V. S. Lebedev, *J. Russ. Laser Res.*, **36**, 175 (2015); DOI: 10.1007/s10946-015-9491-2
15. A. D. Kondorskiy, V. S. Lebedev, *J. Russ. Laser Res.*, **42**, 697 (2021); DOI: 10.1007/s10946-021-10012-3
16. L. Scarabelli, M. Coronado-Puchau, J. J. Giner-Casares, et al., *ACS Nano*, **8**, 5833 (2014); DOI: 10.1021/nn500727w
17. L. Scarabelli, L. M. Liz-Marzán, *ACS Nano*, **15**, 18600 (2021); DOI: 10.1021/acsnano.1c10538
18. N. Takeshima, K. Sugawa, H. Tahara, et al., *Nanoscale Res. Lett.*, **15**, 15 (2020); DOI: 10.1186/s11671-020-3248-8
19. Y. Wang, X. Li, A. Wang, et al., *AJOP*, **9**, 18 (2021); DOI: 10.11648/j.ajop.20210901.13
20. A. D. Kondorskiy, N. T. Lam, and V. S. Lebedev, *J. Russ. Laser Res.*, **39**, 56 (2018); DOI: 10.1007/s10946-018-9689-1
21. N. T. Lam, A. D. Kondorskiy, and V. S. Lebedev, *Bull. Lebedev Phys. Inst.*, **46**, 390 (2019); DOI: 10.3103/S1068335619120066
22. S. Thakur, S. M. Borah, A. Singh, et al., *J. Electron. Mater.*, **52**, 4878 (2023); DOI: 10.1007/s11664-023-10422-w
23. E. C. Le Ru and P. G. Etchegoin, *Principles of Surface Enhanced Raman Spectroscopy and Related Plasmonic Effects*, Elsevier, Amsterdam (2009).
24. H. Kuwata, H. Tamaru, K. Esumi, et al., *Appl. Phys. Lett.*, **83**, 4625 (2003); DOI: 10.1063/1.1630351
25. R. Yu, L. M. Liz-Marzán, and F. J. García de Abajo, *Chem. Soc. Rev.*, **46**, 6710 (2017); DOI: 10.1039/C6CS00919K
26. N. G. Khlebtsov, S. V. Zarkov, V. A. Khanadeeva, and Yu. A. Avetisyan, *Nanoscale*, **12**, 19963 (2020); DOI: 10.1039/d0nr02531c
27. `github.com/kondorskiy/triangle`
28. B. I. Shapiro, E. S. Tyshkunova, A. D. Kondorskiy, and V. S. Lebedev, *Quantum Electron.*, **45**, 1153 (2015); DOI: 10.1070/qe2015v045n12abeh015869
29. U. Kreibig, *J. Phys. F: Metal Phys.*, **4**, 999 (1974); DOI: 10.1088/0305-4608/4/7/007
30. U. Kreibig and M. Vollmer, *Optical Properties of Metal Clusters*, Springer, Berlin/Heidelberg (1995).
31. P. B. Johnson and R. W. Christy, *Phys. Rev. B*, **6**, 4370 (1972); DOI: 10.1103/PhysRevB.6.4370
32. R. L. Olmon, B. Slovick, T. W. Johnson, et al., *Phys. Rev. B*, **86**, 235147 (2012); DOI: 10.1103/PhysRevB.86.235147
33. E. D. Palik (Ed.), *Handbook of Optical Constants of Solids*, Academic, San Diego (1991), Vol. II.